BIOCHEMISTRY
including biophysical chemistry & molecular biology
Article

Biochemistry **2010,** *49,* 9113–9119 9113
DOI: 10.1021/bi1011628

Design of High-Activity Mutants of Human Butyrylcholinesterase against (−)-Cocaine: Structural and Energetic Factors Affecting the Catalytic Efficiency[†]

Fang Zheng, Wenchao Yang, Liu Xue, Shurong Hou, Junjun Liu, and Chang-Guo Zhan*

Department of Pharmaceutical Sciences, College of Pharmacy, University of Kentucky, 789 South Limestone, Lexington, Kentucky 40536, United States

Received July 21, 2010; Revised Manuscript Received August 27, 2010

ABSTRACT: The present study was aimed to explore the correlation between the protein structure and catalytic efficiency of butyrylcholinesterase (BChE) mutants against (−)-cocaine by modeling the rate-determining transition state (TS1), i.e., the transition state for the first step of chemical reaction process, of (−)-cocaine hydrolysis catalyzed by various mutants of human BChE in comparison with the wild type. Molecular modeling of the TS1 structures revealed that mutations on certain nonactive site residues can indirectly affect the catalytic efficiency of the enzyme against (−)-cocaine through enhancing or weakening the overall hydrogen bonding between the carbonyl oxygen of (−)-cocaine benzoyl ester and the oxyanion hole of the enzyme. Computational insights and predictions were supported by the catalytic activity data obtained from wet experimental tests on the mutants of human BChE, including five new mutants reported for the first time. The BChE mutants with at least ∼1000-fold improved catalytic efficiency against (−)-cocaine compared to the wild-type BChE are all associated with the TS1 structures having stronger overall hydrogen bonding between the carbonyl oxygen of (−)-cocaine benzoyl ester and the oxyanion hole of the enzyme. The combined computational and experimental data demonstrate a reasonable correlation relationship between the hydrogen-bonding distances in the TS1 structure and the catalytic efficiency of the enzyme against (−)-cocaine.

Cocaine is a widely abused drug (*1*−*3*) without an FDA[1]-approved medication. The disastrous medical and social consequences of cocaine abuse have made a high priority the development of a medication for treatment of cocaine overdose and addiction (*4*, *5*). It has been recognized an ideal anti-cocaine medication to accelerate cocaine metabolism producing biologically inactive metabolites via a route similar to the primary cocaine-metabolizing pathway, i.e., cocaine hydrolysis catalyzed by butyrylcholinesterase (BChE) in plasma (*4*, *6*−*16*). Unfortunately, wild-type BChE has a low catalytic efficiency against naturally occurring (−)-cocaine (k_{cat} = 4.1 min^{-1} and K_M = 4.5 μM) (*17*−*21*). For development of an anti-cocaine medication, it is interesting to design a mutant of human BChE, which may be regarded as a cocaine hydrolase (CocH), with a significantly improved catalytic activity against (−)-cocaine.

It has been known that computational design of a high-activity enzyme mutant is extremely challenging, particularly when the chemical reaction process is rate-determining for the enzymatic reaction (*22*−*24*). In general, for computational design of a mutant enzyme with an improved catalytic activity for a given substrate, one needs to design possible mutations that can accelerate the rate-determining step of the catalytic reaction process (*18*, *25*, *26*) while the other steps are not slowed down by the mutations. The detailed catalytic reaction pathway for BChE-catalyzed hydrolysis of (−)-cocaine was uncovered by extensive molecular dynamics (MD) simulations (*18*, *25*) and reaction coordinate calculations (*25*, *26*) using quantum mechanics (QM) and hybrid quantum mechanics/molecular mechanics (QM/MM). It has been known (*18*, *22*, *25*, *27*) that the rate-determining step of (−)-cocaine hydrolysis catalyzed by the A328W/Y332A and A328W/Y332G mutants is the first step of the chemical reaction process, although the rate-determining step of (−)-cocaine hydrolysis catalyzed by wild-type BChE is the rotation from the nonprereactive BChE−(−)-cocaine complex to the prereactive BChE−(−)-cocaine complex. Therefore, starting from the A328W/Y332A or A328W/Y332G mutant, rational design of BChE mutants against (−)-cocaine has been focused on decreasing the energy barrier for the first reaction step without significantly affecting the other reaction steps, and our rational design efforts have led to discovery of promising mutants of human BChE with a considerably improved catalytic efficiency (k_{cat}/K_M) against (−)-cocaine (*27*−*30*).

It deserves to be pointed out that the high activity (k_{cat} = 3060 min^{-1} and K_M = 3.1 μM) (*31*) of our previously discovered

[†]This work was supported by NIH Grants R01 DA013930, R01 DA025100, and R01 DA021416.

*To whom correspondence should be addressed. Voice: 859-323-3943. Fax: 859-323-3575. E-mail: zhan@uky.edu.

[1]Abbreviations: BChE, butyrylcholinesterase; TS1, the transition state for the first step of the chemical reaction process; MD, molecular dynamics; QM, quantum mechanics; QM/MM, hybrid quantum mechanics/molecular mechanics; FDA, U.S. Food and Drug Administration; CocH, cocaine hydrolase; ES, enzyme−substrate complex; RCE, relative catalytic efficiency; E1, wild-type BChE; E2, A328W/Y332A mutant of BChE; E3, A328W/Y332G mutant of BChE; E4, F227A/S287G/A328W/Y332M mutant of BChE; E5, A199S/S287G/A328W/Y332G mutant of BChE; E6, A199S/F227L/S287G/A328W/Y332G mutant of BChE; E7, A199S/F227I/S287G/A328W/Y332G mutant of BChE; E8, A199S/F227V/S287G/A328W/Y332G mutant of BChE; E9, A199S/F227A/S287G/A328W/Y332G mutant of BChE; E10, A199S/S287G/A328W/Y332G/L286I mutant of BChE; E11, A199S/F227A/S287G/A328W/Y332G/F329V mutant of BChE; CTST, classical transition state theory; PME, particle mesh Ewald; rmsd, root-mean-square deviation; DMEM, Dulbecco's modified Eagle's medium; TMB, 3,3′,5,5′-tetramethylbenzidine.

Published on Web 10/01/2010

A199S/S287G/A328W/Y332G mutant (*27*) against (−)-cocaine has been validated *in vitro* and *in vivo* by Brimijoin et al. (*32*), who concluded that this mutant is "a true CocH with a catalytic efficiency that is 1,000-fold greater than wild-type BChE" (*32*). Fusing this BChE mutant at its C-terminus with human serum albumin to extend the plasma half-life of the enzyme, Brimijoin et al. found that the A199S/S287G/A328W/Y332G mutant (*27*) (or CocH in their notation) fused with human serum albumin can selectively block cocaine toxicity and reinstatement of drug seeking in rats (*32*). The extensive experimental data reported by Brimijoin et al. (*32*) strongly supported the potential therapeutic value of our designed and discovered A199S/S287G/A328W/Y332G mutant (*27*) of human BChE, and they concluded that the treatment with this mutant (fused with human serum albumin) "was well tolerated and may be worth exploring for clinical application in humans" (*32*). *In vivo* studies described in our previous report (*29*) also revealed that the A199S/F227A/S287G/A328W/Y332G mutant of human BChE, without fusing with any other protein, can also efficiently protect mice from the acute toxicity of a lethal dose of cocaine (180 mg/kg). All of the encouraging *in vivo* activity data (*29*, *32*, *33*) concerning our designed and discovered high-activity mutants of human BChE inspired us to continue rational design and discovery of new mutants of human BChE with a further improved catalytic efficiency against (−)-cocaine.

For rational design of new mutants of BChE with a further improved catalytic efficiency against (−)-cocaine, it is important to explore the major factors affecting the catalytic efficiency of BChE mutants and understand the correlation between the protein structure and catalytic efficiency for the mutants against (−)-cocaine. In the present study, we aimed to explore the structure−activity correlation by modeling the rate-determining transition state (TS1), i.e., the transition state for the first step of chemical reaction process (see Figure 1), of (−)-cocaine hydrolysis catalyzed by various mutants of human BChE in comparison with the wild-type enzyme. Computational modeling and predictions were followed by wet experimental tests to determine the actual catalytic efficiency of the BChE mutants against (−)-cocaine. The combined computational and experimental data demonstrate a reasonable correlation relationship between the calculated enzyme−(−)-cocaine hydrogen-bonding distances in the TS1 structure and the measured catalytic efficiency of the enzyme against (−)-cocaine.

MATERIALS AND METHODS

Computational Modeling. The general strategy of performing an energy minimization or MD simulation on a transition state structure of an enzymatic reaction using a classical force field (molecular mechanics) has been described and justified in our recent studies (*22*−*30*). Molecular modeling of the TS1 structures associated with various mutants of human BChE was based on the TS1 geometry determined in our previously reported molecular modeling and reaction coordinate calculation (*29*) on (−)-cocaine hydrolysis catalyzed by the A199S/F227A/S287G/A328W/Y332G mutant of human BChE; the molecular modeling started from the X-ray crystal structure (*34*) deposited in the Protein Data Bank (PDB code 1POP), and the reaction coordinate calculation was carried out by using a hybrid quantum mechanical/molecular mechanical (QM/MM) approach in which the QM part was treated at the B3LYP/6-31G* level and the MM part was treated by using Amber force field (version ff99).

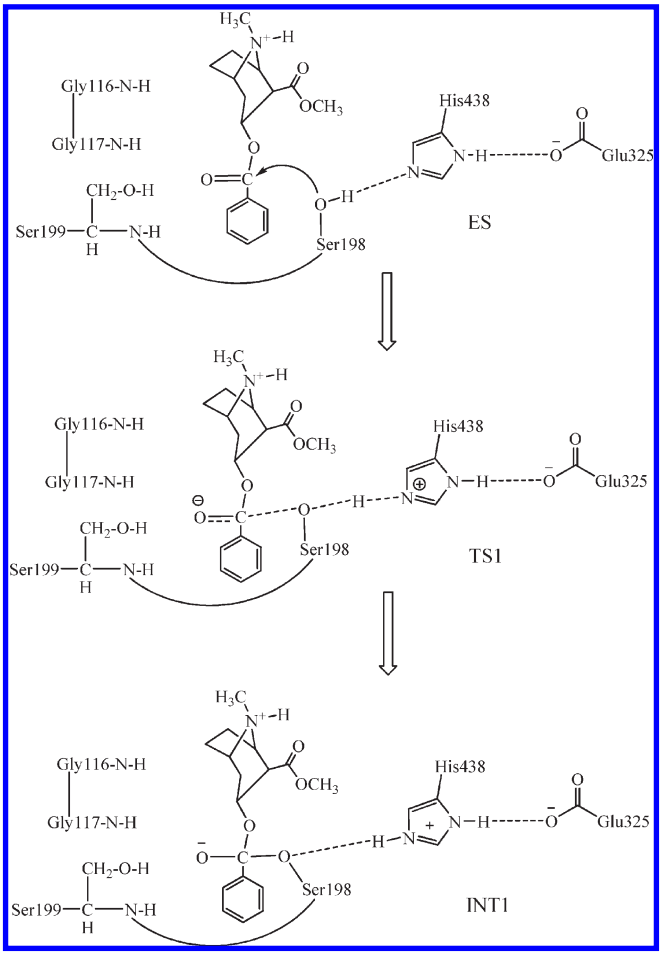

FIGURE 1: Schematic representation of the first reaction step of the chemical reaction process for (−)-cocaine hydrolysis catalyzed by BChE mutant including the A199S mutation.

Starting from the QM/MM-optimized TS1 geometry (*29*), we used Amber9 package (*35*) to model the TS1 structures associated with all BChE mutants and the wild-type involved in the present study.

In order to be consistent with our previous studies on this enzyme, the ff99 force field parameters were used for all standard amino acid residues of BChE, whereas the (−)-cocaine and other residues (His438 and Glu325) involved in the reaction center were considered as the nonstandard residues and parametrized in the same way described in our previous report (*29*). The partial atomic charges of the nonstandard residues in the TS1 structures were calculated by using the RESP protocol implemented in the Antechamber module of the Amber9 program (*35*) following electrostatic potential (ESP) calculations at *ab initio* HF/6-31G* level using the Gaussian03 program (*36*).

The general strategy of modeling a transition state structure of an enzymatic reaction using an Amber force field or another classical force field (molecular mechanism) has been described and justified in our recent studies (*27*, *29*). In principle, energy minimization (or molecular dynamics simulation) using an Amber force field can only model a stable structure corresponding to a local minimum on the potential energy surface, whereas a transition state during a reaction process is always associated with a first-order saddle point on the potential energy surface. Hence, one cannot energy-minimize a transition state structure by using an Amber force field without any restraint on the geometry of the transition state. Nevertheless, if we can

technically remove a vibrational degree of freedom associated with the imaginary vibration in the transition state structure, then the number of the vibrational degrees of freedom (normal vibration modes) for a nonlinear molecule will decrease from $3N - 6$. The transition state structure is associated with a local minimum on the potential energy surface within a subspace of the reduced vibrational degrees of freedom, although it is associated with a first-order saddle point on the potential energy surface with all of the $3N - 6$ vibrational degrees of freedom. Theoretically, the vibrational degree of freedom associated with the imaginary vibrational frequency in the transition state structure can be removed by appropriately freezing the reaction coordinate. The reaction coordinate corresponding to the imaginary vibration of the transition state is generally characterized by a combination of some key geometric parameters. These key geometric parameters are usually bond lengths of the transition bonds, i.e., the forming and breaking covalent bonds during the specific reaction step under consideration (see below for the specific transition bonds involved in this work). Thus, one just needs to maintain the lengths of the transition bonds during the energy minimization of a transition state structure.

For each TS1 structure involved in this study, the system was neutralized and solvated in a rectangular box of TIP3P water molecule (*37*) with a minimum solute−wall distance of 10 Å. The solvent water molecules and counterions in the solvated systems were carefully equilibrated and energy-minimized first, and then the entire system was energy-minimized until convergence by using the Sander module of Amber9 program with a convergence criterion of 0.01 kcal mol^{-1} $Å^{-1}$. For each energy minimization job, we used steepest descent method for the first 1000 steps, and then it was switched to conjugate gradient method until the convergence. During the energy minimization on the entire system, only the lengths of the transition bonds (i.e., the gradually forming/breaking covalent bonds during the reaction step) were restrained. Specifically, there are a total of three transition bonds in the modeled TS1 structure: partial covalent bond between the carbonyl carbon of (−)-cocaine and the hydroxyl oxygen of S198 side chain (the optimized transition bond length: 1.93 Å); partial covalent bond between the oxygen and hydrogen atoms of the hydroxyl group of S198 side chain (the optimized transition bond length: 1.43 Å); partial covalent bond between the hydroxyl hydrogen of S198 side chain and the nitrogen (N^{ϵ}) atom of H438 side chain (the optimized transition bond length: 1.13 Å). The particle mesh Ewald (PME) method (*38*) was used to treat long-range electrostatic interactions. Ten angstroms was used as the nonbonded cutoff. The energy-minimized TS1 structures were used to obtain the key internuclear distances required in this work.

Experimental Studies. Cloned *pfu* DNA polymerase and *Dpn*I endonuclease were obtained from Stratagene (La Jolla, CA). [^{3}H]-(−)-cocaine (50 Ci/mmol) was purchased from Perkin-Elmer Life Sciences (Boston, MA). All oligonucleotides were synthesized by the Integrated DNA Technologies, Inc. (Coralville, IA). The QIAprep spin plasmid miniprep kit and Qiagen plasmid purification kit and QIAquick PCR purification kit were obtained from Qiagen (Santa Clarita, CA). Human embryonic kidney 293T/17 cells were from ATCC (Manassas, VA). Dulbecco's modified Eagle's medium (DMEM) was purchased from Fisher Scientific (Fairlawn, NJ). 3,3′,5,5′-Tetramethylbenzidine (TMB) was obtained from Sigma (St. Louis, MO). Anti-BChE (mouse monoclonal antibody, product no. HAH002-01) was purchased from AntibodyShop (Gentofte, Denmark), and goat anti-mouse IgG HRP conjugate was from Zymed (San Francisco, CA).

Site-directed mutagenesis of human BChE cDNA was performed by using the QuikChange method (*39*). Further mutation(s) required to produce a new BChE mutant cDNA was (were) generated from the cDNA corresponding to the A199S/S287G/A328W/Y332G mutant of human BChE in a pRc/CMV expression plasmid (*40*). Using plasmid DNA as template and primers with specific base pair alterations, mutations were made by polymerase chain reaction with *Pfu* DNA polymerase for replication fidelity. The PCR product was treated with *Dpn*I endonuclease to digest the parental DNA template. Modified plasmid DNA was transformed into *Escherichia coli*, amplified, and purified. The DNA sequences of the mutants were confirmed by DNA sequencing.

Both the wild type and mutants of human BChE were expressed, and their enzyme activity against (−)-cocaine was assayed at the same time under the same experimental conditions; the wild type was used as a standard reference. The proteins (wild type and mutants of BChE) were expressed in human embryonic kidney cell line 293T/17. Cells were grown to 80−90% confluence in six-well dishes and then transfected by Lipofectamine 2000 complexes of 4 μg of plasmid DNA per each well. Cells were incubated at 37 °C in a CO_2 incubator for 24 h, and cells were moved to a 60 mm culture vessel and cultured for an additional 4 days. The culture medium [10% fetal bovine serum in Dulbecco's modified Eagle's medium (DMEM)] was harvested for the BChE activity assays.

To measure (−)-cocaine and benzoic acid, the product of (−)-cocaine hydrolysis catalyzed by BChE, we used sensitive radiometric assays based on toluene extraction of [^{3}H]-(−)-cocaine labeled on its benzene ring (*41*). In brief, to initiate the enzymatic reaction, 100 nCi of [^{3}H]-(−)-cocaine was mixed with 100 μL of culture medium. The enzymatic reactions proceeded at room temperature (25 °C) with varying concentrations of (−)-cocaine. The reactions were stopped by adding 300 μL of 0.02 M HCl, which neutralized the liberated benzoic acid while ensuring a positive charge on the residual (−)-cocaine. [^{3}H]Benzoic acid was extracted by 1 mL of toluene and measured by scintillation counting. Finally, the measured (−)-cocaine concentration-dependent radiometric data were analyzed by using the standard Michaelis−Menten kinetics so that the catalytic parameters were determined along with the use of an enzyme-linked immunosorbent assay (ELISA) protocol (*29*).

RESULTS AND DISCUSSION

Energy-Minimized TS1 Structures and Hydrogen-Bonding Distances. We modeled the TS1 structures for (−)-cocaine hydrolysis catalyzed by wild-type BChE (E1) and its various mutants. Summarized in Table 1 are important geometric parameters related to hydrogen bonding in the modeled TS1 structures. We will first discuss the results calculated for E1 and eight representative mutants, including A328W/Y332A (E2), A328W/Y332G (E3), F227A/S287G/A328W/Y332A (AME359 or E4) and five other mutants containing the A199S/S287G/A328W/Y332G mutations (E5 to E9). The modeled TS1 structures revealed a total of four potential enzyme−(−)-cocaine hydrogen bonds, all with the carbonyl oxygen of (−)-cocaine benzoyl ester. The four potential hydrogen bonds may be characterized by the H···O distances D1 to D4 listed in Table 1. Specifically, D1, D2, and D3 represent the internuclear distances between the carbonyl

Table 1: Calculated Key Internuclear Distances (D1−D4) between (−)-Cocaine and the Oxyanion Hole (Consisting of Residues 116, 117, and 199) in the Modeled First Transition State (TS1)

enzyme		internuclear distance[a]			
ID	mutation	D1	D2	D3	D4
E1	wild-type BChE	2.63	2.05	1.95	N/A
E2	A328W/Y332A	2.91	1.97	2.01	N/A
E3	A328W/Y332G	2.92	1.94	1.98	N/A
E4	F227A/S287G/A328W/Y332M (AME359)	2.86	1.95	1.95	N/A
E5	A199S/S287G/A328W/Y332G	2.86	2.05	1.71	1.95
E6	A199S/F227L/S287G/A328W/Y332G	2.83	2.02	1.73	1.92
E7	A199S/F227I/S287G/A328W/Y332G	2.90	2.01	1.71	1.93
E8	A199S/F227V/S287G/A328W/Y332G	2.91	2.03	1.71	1.92
E9	A199S/F227A/S287G/A328W/Y332G	2.94	1.98	1.71	1.92
E10	A199S/S287G/A328W/Y332G/L286I	2.61	2.09	1.72	2.01
E11	A199S/F227A/S287G/A328W/Y332G/F329V	3.01	2.06	1.77	1.97

[a]D1, D2, and D3 represent the internuclear distances between the carbonyl oxygen of (−)-cocaine benzoyl ester and the NH hydrogen of residues 116 (i.e., G116), 117 (i.e., G117), and 199 (i.e., A199 or S199) of BChE, respectively, in the modeled TS1 structure. D4 is the internuclear distance between the carbonyl oxygen of (−)-cocaine benzoyl ester and the hydroxyl hydrogen of the S199 side chain in the mutants containing the A199S mutation.

oxygen of (−)-cocaine benzoyl ester and the NH hydrogen of G116, G117, and A199 (or S199) of BChE, respectively. D4 is the internuclear distance between the carbonyl oxygen of (−)-cocaine benzoyl ester and the hydroxyl hydrogen of the S199 side chain in the mutants containing the A199S mutation. As shown in Table 1, the simulated H···O distance D1 is always too long for the peptidic NH of G116 to form a really significant N−H···O hydrogen bond with the carbonyl oxygen of (−)-cocaine in all of the simulated TS1 structures.

Compared to wild-type BChE (E1), mutant enzymes E2 to E4 all have a smaller D2 value which means a shorter and stronger hydrogen bond between the carbonyl oxygen of (−)-cocaine benzoyl ester and the NH group of G117 backbone. Correspondingly, these mutants have an improved catalytic efficacy of E2 to E4 compared to E1. Compared to E2 to E4, the other BChE mutants (E5 to E9) listed in Table 1 have shorter hydrogen bond interactions between the carbonyl oxygen of (−)-cocaine benzoyl ester and residue 199 (i.e., S199), including a significantly shorter hydrogen bond with the S199 backbone NH group (corresponding to D3) and an additional hydrogen bond with the hydroxyl group of S199 side chain (corresponding to D4).

Starting from E5, the further mutation on F227 changes the hydrogen-bonding interactions by mainly adjusting the lengths of three hydrogen bonds associated with D2, D3, and D4, especially that associated with D2, through perturbing the protein structure (including both the backbone and side chains). Compared to E5, whereas E6 to E9 display similar structural patterns associated with D1 to D4, it is notable that E6 to E9 all have a smaller D2 value and, therefore, a stronger hydrogen bond between the carbonyl oxygen of (−)-cocaine benzoyl ester and the NH group of G117 backbone. Based on the values of D2 to D4 listed in Table 1, the overall hydrogen bonding is enhanced in the TS1 structures associated with E7 to E9, compared to the TS1 structure associated with E5; E9 is associated with the most stable TS1 structure compared to all others mutants listed in Table 1.

The results calculated for E1 to E9 revealed an important insight into the computational design of high-activity mutants of the enzyme against (−)-cocaine. F227 residue of BChE is not in the active site, and it is far away from (−)-cocaine. The internuclear distance measured between the Cα atom of F227 residue and the carbonyl carbon of (−)-cocaine benzoyl ester in the TS1 state is ∼12 Å. However, a mutation on F227 can still significantly affect the transition state stabilization and, thus, shift the catalytic efficiency of BChE. This is because mutation on a nonactive site residue, such as F227, could indirectly affect the hydrogen bonding between the oxyanion hole and (−)-cocaine through perturbing the protein environment of the active site. Such kind of structural perturbation could have either beneficial or adverse effects on the catalytic efficiency of the enzyme. Only when all residues in an enzyme cooperate in a way which stabilizes the rate-determining transition state and, thus, lowers the free energy barrier of the enzymatic reaction can the catalytic efficacy of the enzyme be improved. In light of the computational insight, it would be naïve to believe that any mutation based on E5 or E9 will keep or further improve the catalytic efficiency of the mutant enzyme. In contrast, many mutations would decrease the catalytic efficiency of the mutant. For example, the L286I mutation on E5 produces E10 and the F329V mutation on E9 results in E11. Both the L286I mutation on E5 and F329V mutation on E9 weaken the overall hydrogen bonding between the oxyanion hole and (−)-cocaine in the modeled TS1 structures and, thus, destabilize the TS1 structures compared to the corresponding parent mutants (i.e., E5 for E10 and E9 for E11), as seen in Table 1.

Experimental Kinetic Data. To examine the above computational insights and predictions, all of the new mutants of human BChE listed in Table 1 were produced through site-directed mutagenesis and protein expression. For comparison, wild-type BChE and its high-activity mutants (E5 to E9) listed in Table 2 were expressed, and their catalytic activity against (−)-cocaine was assayed at the same time under the same experimental conditions. On the basis of the kinetic analysis, we have determined the catalytic efficiency of each new mutant against (−)-cocaine compared to wild-type BChE. Summarized in Table 2 are experimental kinetic data for E1 and E9 in comparison with the calculated results.

As summarized in Table 2, E5 to E9 all have an ∼1000- to ∼2000-fold improved catalytic efficiency (k_{cat}/K_M) against (−)-cocaine compared to the wild type. The considerably improved catalytic efficiency of E5 to E9 is consistent with the significantly shortened hydrogen bonds calculated for these mutants. Compared to E5 (a proven promising therapeutic candidate in anti-cocaine medication development (*32*)) in which F227 is not mutated, the other four mutants (i.e., E6 to E9) with mutations on F227 have a further improved catalytic efficiency against (−)-cocaine. All of these high-activity mutants (E5 to E9) may be considered as promising candidates in the development of an anti-cocaine medication. Both the computational and experimental data consistently indicate that the highest catalytic efficiency is associated with E9.

Further, we examined other two mutants (E10 and E11) corresponding to the L286I mutation on E5 and the F329V mutation on E9. With the relatively longer hydrogen bonds in overall (see Table 1), the L286I mutation on E5 and the F329V mutation on E9 were all predicted to decrease the catalytic efficiency of the mutant against (−)-cocaine. According to the experimental data in Table 3, the L286I mutation on

Table 2: Experimental Kinetic Parameters in Comparison with the Calculated Relative Catalytic Activity (RCE) Data for (−)-Cocaine Hydrolysis Catalyzed by Wild-Type BChE and Its Mutants

enzyme (wild-type BChE or its mutant)		exptl			calcd
ID	mutation	k_{cat}/K_M (min^{-1} M^{-1})	RCE[a]	ln(RCE)	ln(RCE)[f]
E1	wild-type BChE[b]	9.1×10^5	1	0.00	1.74
E2	A328W/Y332A[c]	8.5×10^6	9.4	2.24	1.84 (2.46)
E3	A328W/Y332G[d]	1.4×10^7	15	2.71	2.17 (2.75)
E4	F227A/S287G/A328W/Y332M (AME359)[e]	3.1×10^7	34	3.53	2.30 (2.86)
E5	A199S/S287G/A328W/Y332G	9.9×10^8	1080	6.98	6.90 (6.87)
E6	A199S/F227L/S287G/A328W/Y332G	1.0×10^9	1130	7.03	6.77 (6.75)
E7	A199S/F227I/S287G/A328W/Y332G	1.1×10^9	1170	7.06	7.14 (7.07)
E8	A199S/F227V/S287G/A328W/Y332G	1.4×10^9	1490	7.31	7.19 (7.12)
E9	A199S/F227A/S287G/A328W/Y332G	1.8×10^9	2020	7.61	7.44 (7.34)

[a]RCE refers to the relative catalytic efficiency (k_{cat}/K_M), i.e., the ratio of the k_{cat}/K_M value of the enzyme to that of wild-type BChE (E1) against (−)-cocaine. [b]Data from ref 41. [c]Data from ref 41. [d]Data from ref *28*. [e]Data from ref 11. [f]Calculated by using eq 4. The values in parentheses are calculated by using eq 5.

Table 3: Predicted and Observed Effects of the L286I and F329V Mutations on the Catalytic Activity of E5 and E9, Respectively

BChE mutant		exptl[a]		calcd	
ID	mutation	RCE[b]	ln(RCE)	Cα−COC (Å)[c]	ln(RCE)[d]
E5	A199S/S287G/A328W/Y332G	1080	6.98	8.0	6.90 (6.87)
E10	A199S/S287G/A328W/Y332G/L286I	242	5.49	8.3	6.02 (6.10)
E9	A199S/F227A/S287G/A328W/Y332G	2020	7.61	10.4	7.44 (7.34)
E11	A199S/F227A/S287G/A328W/Y332G/F329V	121	4.80	10.2	5.24 (5.42)

[a]Experimental activity data for E10 and E11 were estimated by performing kinetic analysis using 5 μM (−)-cocaine. [b]Relative catalytic efficiency of the enzyme (relative to that of E1) against (−)-cocaine. [c]The distance between the carbonyl carbon of (−)-cocaine benzoyl ester and the Cα atom of the residue for the additional mutation, i.e., 286 (for E5 and E10) or 329 (for E9 and E11). [d]Calculated by using eq 4. The values in parentheses are calculated by using eq 5.

E5 decreased the catalytic efficiency of E5 by ~5-fold, and the F329V mutation on E9 decreased the catalytic efficiency of E9 by ~17-fold. All of the experimental kinetic data are qualitatively consistent with the computational predictions.

Quantitative Correlation Relationship between the Hydrogen-Bonding Distances and the Catalytic Efficiency of BChE Mutant against (−)-Cocaine. In light of the encouraging agreement between the computational and experimental data discussed above, we wanted to know whether it is possible to develop a quantitative correlation relationship between the calculated hydrogen-bonding distances (D2 to D4) and the experimental catalytic efficiency of the enzyme against (−)-cocaine. Theoretically, the catalytic efficiency (k_{cat}/K_M) of an enzyme for a substrate is dependent on the free energy change from the free enzyme (E) and free substrate (S) to the rate-determining transition state (TS1 in the present work), denoted by ΔG(E+S→TS1). For a series of BChE mutants, assuming that the relative magnitudes of ΔG(E+S→TS1) are mainly affected by the overall hydrogen bonding discussed above, we should have the following empirical correlation relationship:

$$\ln(k_{cat}/K_M) = af(D,n) + b' \quad (1)$$

When the relative catalytic efficiency (RCE) is used, eq 1 becomes

$$\ln(\mathrm{RCE}) \equiv \ln\left[\frac{(k_{cat}/K_M)_{mutant}}{(k_{cat}/K_M)_{wild\ type}}\right] = af(D,n) + b \quad (2)$$

In eqs 1 and 2, a, b', and b are all constants for a series of BChE mutants with $b = b' - \ln(k_{cat}/K_M)_{wild\ type}$, and $f(D,n)$ is a generally defined function (descriptor) which will be chosen to reflect the overall hydrogen bonding between the carbonyl oxygen of (−)-cocaine benzoyl ester and the oxyanion hole of the enzyme. In the present study, $f(D,n)$ is defined as follows:

$$f(D,n) = \frac{1}{D2^n} + \frac{1}{D3^n} + \frac{1}{D4^n} \quad (3)$$

in which n is an empirical parameter (an integer) to be fitted. The actual value of n might be determined by the nature of the interactions. For example, $n = 1$ would suggest that the main interactions are electrostatic. We expect $n > 1$ for mainly nonelectrostatic interactions. For the enzymes (including E1 to E4) where D4 is not applicable, D4 in eq 4 is considered to be infinite (D4 = ∞) such that 1/D4 = 0.

For a preliminary practical test of eqs 2 and 3, the empirical parameters n, a, and b were determined by the least-squares fitting to the corresponding experimental ln(RCE) values for all of the 11 enzymes (E1 to E11) examined in this study. Through the least-squares fitting, we obtained

$$\ln(\mathrm{RCE}) = 633.7f(D,9) - 0.806 \quad (4)$$

with a high linear correlation coefficient of $R = 0.96$ and a root-mean-square deviation (rmsd) of 0.71. In eq 4, $n = 9$, suggesting that the interactions involving D2 to D4 are mainly nonelectrostatic. The ln(RCE) values calculated by using eq 4 are listed in Tables 2 and 3 for comparison with the corresponding experimental ln(RCE) values. As seen in Tables 2 and 3, the calculated ln(RCE) values are reasonably close to the corresponding experimental data on the whole. The deviations of the calculated ln(RCE) values from the experimental data can be attributed to many other factors (beyond the hydrogen binding between

(−)-cocaine and the oxyanion hole) that have not been accounted for in eq 2. Nevertheless, the satisfactory correlation (R = 0.96 and rmsd = 0.71) between the $f(D,9)$ and ln(RCE) values clearly demonstrates that the enzyme−substrate hydrogen-bonding interactions are indeed the primary factor affecting the catalytic efficiency of the BChE mutants against (−)-cocaine.

Further, within the ln(RCE) values calculated by using eq 4 for the 11 enzymes, the largest deviation is associated with E1 (wild-type BChE). Equation 4 overestimates the ln(RCE) value of E1 by 1.74. This is not surprising in consideration of the fact that the rate-determining step of (−)-cocaine hydrolysis catalyzed by wild-type BChE (E1) is the (−)-cocaine rotation from the nonprereactive BChE−(−)-cocaine complex to the prereactive BChE−(−)-cocaine complex (*25*), instead of the first step of the chemical reaction process. So, the actual catalytic efficiency of E1 should be significantly lower than that predicted from eq 2 or 4 which was based on the preassumption that the first step of the chemical reaction process is rate-determining.

Excluding E1, when the least-squares fitting was applied to only the BChE mutants (E2 to E11), we obtained

$$\ln(\mathrm{RCE}) = 551.2f(D,9) + 0.163 \quad (5)$$

with R = 0.98 and rmsd = 0.39. Equation 5 looks more reasonable, as the rmsd value of 0.39 for eq 5 is significantly smaller than that of 0.71 for eq 4. The ln(RCE) values calculated by using eq 5 are also listed in Tables 2 and 3 for comparison. As seen in Tables 2 and 3, the overall agreement between the computational and experimental ln(RCE) values becomes better when eq 5 is used instead of eq 4.

CONCLUSION

Molecular modeling of the rate-determining transition state (TS1), i.e., the transition state for the first step of chemical reaction process, of (−)-cocaine hydrolysis catalyzed by various mutants of human BChE in comparison with wild-type BChE revealed that certain mutations on nonactive site residues (even if they are far away from the reaction center) can indirectly affect the catalytic efficiency of the enzyme against (−)-cocaine through enhancing/weakening the overall hydrogen bonding between the carbonyl oxygen of (−)-cocaine benzoyl ester and the oxyanion hole of the enzyme in the TS1 structure. The computational insights and predictions were supported by the results obtained from wet experimental tests on the mutants of human BChE. All of the high-activity mutants, i.e., those with at least ∼1000-fold improved catalytic efficiency against (−)-cocaine compared to the wild type, are indeed associated with the TS1 structures having stronger overall hydrogen bonding between the carbonyl oxygen of (−)-cocaine benzoyl ester and the oxyanion hole of the enzyme. All of these high-activity mutants (E5 to E9) may be considered as promising candidates in anti-cocaine medication development. The combined computational and experimental data demonstrate a reasonable correlation relationship between the calculated hydrogen-bonding distances in the TS1 structure and the measured catalytic efficiency of the enzyme against (−)-cocaine. The general concept of the computational design of BChE mutants and the correlation between the catalytic efficiency of an enzyme and the structural parameters in the rate-determining transition state may also be useful in studying catalytic mechanisms of other enzymes and factors affecting their catalytic efficiency.

ACKNOWLEDGMENT

The authors acknowledge the Center for Computational Sciences (CCS) at the University of Kentucky for supercomputing time on an IBM X-series supercomputer cluster with 340 nodes or 1360 processors.

REFERENCES

1. Mendelson, J. H., and Mello, N. K. (1996) Management of cocaine abuse and dependence. *New Engl. J. Med. 334*, 965–972.
2. Singh, S. (2000) Chemistry, design, and structure-activity relationship of cocaine antagonists. *Chem. Rev. 100*, 925–1024.
3. Paula, S., Tabet, M. R., Farr, C. D., Norman, A. B., and Ball, W. J., Jr. (2004) Three-dimensional quantitative structure-activity relationship modeling of cocaine binding by a novel human monoclonal antibody. *J. Med. Chem. 47*, 133–142.
4. Gorelick, D. A. (1997) Enhancing cocaine metabolism with butyrylcholinesterase as a treatment strategy. *Drug Alcohol Depend. 48*, 159–165.
5. Redish, A. D. (2004) Addiction as a computational process gone awry. *Science 306*, 1944–1947.
6. Meijler, M. M., Kaufmann, G. F., Qi, L. W., Mee, J. M., Coyle, A. R., and Moss, J. A. (2005) Fluorescent cocaine probes: a tool for the selection and engineering of therapeutic antibodies. *J. Am. Chem. Soc. 127*, 2477–2484.
7. Carrera, M. R. A., Kaufmann, G. F., Mee, J. M., Meijler, M. M., Koob, G. F., and Janda, K. D. (2004) Treating cocaine addiction with viruses. *Proc. Natl. Acad. Sci. U.S.A. 101*, 10416–10421.
8. Landry, D. W., Zhao, K., Yang, G.X-Q., Glickman, M., and Georgiadis, T. M. (1993) Antibody-catalyzed degradation of cocaine. *Science 259*, 1899–1901.
9. Zhan, C.-G., Deng, S.-X., Skiba, J. G., Hayes, B. A., Tschampel, S. M., Shields, G. C., and Landry, D. W. (2005) First-principle studies of intermolecular and intramolecular catalysis of protonated cocaine. *J. Comput. Chem. 26*, 980–986.
10. Kamendulis, L. M., Brzezinski, M. R., Pindel, E. V., Bosron, W. F., and Dean, R. A. (1996) Metabolism of cocaine and heroin is catalyzed by the same human liver carboxylesterases. *J. Pharmacol. Exp. Ther. 279*, 713–717.
11. Gao, Y., Atanasova, E., Sui, N., Pancook, J. D., Watkins, J. D., and Brimijoin, S. (2005) Gene transfer of cocaine hydrolase suppresses cardiovascular responses to cocaine in rats. *Mol. Pharmacol. 67*, 204–211.
12. Zhan, C.-G. (2009) Novel pharmacological approaches to treatment of drug overdose and addiction. *Expert Rev. Clin. Pharmacol. 2*, 1–4.
13. Zheng, F., and Zhan, C.-G. (2009) Recent progress in protein drug design and discovery with a focus on novel approaches to the development of anti-cocaine medications. *Future Med. Chem. 1*, 515–528.
14. Gao, D., Narasimhan, D. L., Macdonald, J., Ko, M.-C., Landry, D. W., Woods, J. H., Sunahara, R. K., and Zhan, C.-G. (2009) Thermostable variants of cocaine esterase for long-time protection against cocaine toxicity. *Mol. Pharmacol. 75*, 318–323.
15. Collins, G. T., Brim, R. L., Narasimhan, D., Ko, M.-C., Sunahara, R. K., Zhan, C.-G., and Woods, J. H. (2009) Cocaine esterase prevents cocaine-induced toxicity and the ongoing intravenous self-administration of cocaine in rats. *J. Pharmacol. Exp. Ther. 331*, 445–455.
16. Brim, R. L., Nance, M. R., Youngstrom, D. W., Narasimhan, D., Zhan, C.-G., Tesmer, J. J. G., Sunahara, R. K., and Woods, J. H. (2010) A thermally stable form of bacterial cocaine esterase: a potential therapeutic agent for treatment of cocaine abuse. *Mol. Pharmacol. 77*, 593–600.
17. Sun, H., Pang, Y. P., Lockridge, O., and Brimijoin, S. (2002) Re-engineering butyrylcholinesterase as a cocaine hydrolase. *Mol. Pharmacol. 62*, 220–224.
18. Hamza, A., Cho, H., Tai, H.-H., and Zhan, C.-G. (2005) Molecular dynamics simulation of cocaine binding with human butyrylcholinesterase and its mutants. *J. Phys. Chem. B 109*, 4776–4782.
19. Gateley, S. J. (1991) Activities of the enantiomers of cocaine and some related compounds as substrates and inhibitors of plasma butyrylcholinesterase. *Biochem. Pharmacol. 41*, 1249–1254.
20. Darvesh, S., Hopkins, D. A., and Geula, C. (2003) Neurobiology of butyrylcholinesterase. *Nat. Rev. Neurosci. 4*, 131–138.
21. Giacobini, E. (2003) Butyrylcholinesterase: Its Function and Inhibitors, Dunitz Martin, Great Britain.
22. Gao, D., and Zhan, C.-G. (2006) Modeling evolution of hydrogen bonding and stabilization of transition states in the process of cocaine hydrolysis catalyzed by human butyrylcholinesterase. *Proteins 62*, 99–110.

23. Gao, D., and Zhan, C.-G. (2005) Modeling effects of oxyanion hole on the ester hydrolysis catalyzed by human cholinesterases. *J. Phys. Chem. B 109*, 23070–23076.
24. Gao, D., Cho, H., Yang, W., Pan, Y., Yang, G.-F., Tai, H.-H., and Zhan, C.-G. (2006) Computational design of a human butyrylcholinesterase mutant for accelerating cocaine hydrolysis based on the transition-state simulation. *Angew. Chem., Int. Ed. 45*, 653–657.
25. Zhan, C.-G., Zheng, F., and Landry, D. W. (2003) Fundamental reaction mechanism for cocaine hydrolysis in human butyrylcholinesterase. *J. Am. Chem. Soc. 125*, 2462–2474.
26. Zhan, C.-G., and Gao, D. (2005) Catalytic mechanism and energy barriers for butyrylcholinesterase-catalyzed hydrolysis of cocaine. *Biophys. J. 89*, 3863–3872.
27. Pan, Y., Gao, D., Yang, W., Cho, H., Yang, G.-F., Tai, H.-H., and Zhan, C.-G. (2005) Computational redesign of human butyrylcholinesterase for anticocaine medication. *Proc. Natl. Acad. Sci. U.S.A. 102*, 16656–16661.
28. Pan, Y., Gao, D., Yang, W., Cho, H., and Zhan, C.-G. (2007) Free energy perturbation (FEP) simulation on the transition states of cocaine hydrolysis catalyzed by human butyrylcholinesterase and its mutants. *J. Am. Chem. Soc. 129*, 13537–13543.
29. Zheng, F., Yang, W., Ko, M.-C., Liu, J., Cho, H., Gao, D., Tong, M., Tai, H.-H., Woods, J. H., and Zhan, C.-G. (2008) Most efficient cocaine hydrolase designed by virtual screening of transition states. *J. Am. Chem. Soc. 130*, 12148–12155.
30. Yang, W., Pan, Y., Zheng, F., Cho, H., Tai, H.-H., and Zhan, C.-G. (2009) Free energy perturbation (FEP) simulation on transition states and design of high-activity mutants of human butyrylcholinesterase for accelerating cocaine metabolism. *Biophys. J. 96*, 1931–1938.
31. Yang, W., Xue, L., Fang, L., and Zhan, C.-G. (2010) Characterization of a high-activity mutant of human butyrylcholinesterase against (−)-cocaine. *Chem.-Biol. Interact. 187*, 148−152.
32. Brimijoin, S., Gao, Y., and Anker, J. J. (2008) A cocaine hydrolase engineered from human butyrylcholinesterase selectively blocks cocaine toxicity and reinstatement of drug seeking in rats. *Neuropsychopharmacology 33*, 2715–2725.
33. Gao, Y., Orson, F. M., Kinsey, B., Kosten, T., and Brimijoin, S. (2010) The concept of pharmacologic cocaine interception as a treatment for drug abuse. *Chem.-Biol. Interact. 187*, 421−424.
34. Nicolet, Y., Lockridge, O., Masson, P., Fontecilla-Camps, J. C., and Nachon, F. (2003) *J. Biol. Chem. 278*, 41141–41147.
35. Case, D. A., Darden, T. A., Cheatham, T. E., III, Simmerling, C. L., Wang, J. D. R., Luo, R., Merz, K. M., Pearlman, D. A., Crowley, M., Walker, R. C., Zhang, W., Wang, B., Hayik, S., Roitberg, A., Seabra, G., Wong, K. F., Paesani, F., Wu, X., Brozell, S., Tsui, V., Gohlke, H., Yang, L., Tan, C., Mongan, J., Hornak, V., Cui, G., Beroza, P., Mathews, D. H., Schafmeister, C., Ross, W. S., and Kollman, P. A. Amber 9 (2006) University of California, San Francisco, CA.
36. Frisch, M. J., Trucks, G. W., Schlegel, H. B., Scuseria, G. E., Robb, M. A., Cheeseman, J. R., Montgomery, J. A., Jr.,, Vreven, T., Kudin, K. N., Burant, J. C., Millam, J. M., Iyengar, S. S., Tomasi, J., Barone, V., Mennucci, B., Cossi, M., Scalmani, G., Rega, N., Petersson, G. A., Nakatsuji, H., Hada, M., Ehara, M., Toyota, K., Fukuda, R., Hasegawa, J., Ishida, M., Nakajima, T., Honda, Y., Kitao, O., Nakai, H., Klene, M., Li, X., Knox, J. E., Hratchian, H. P., Cross, J. B., Adamo, C., Jaramillo, J., Gomperts, R., Stratmann, R. E., Yazyev, O., Austin, A. J., Cammi, R., Pomelli, C., Ochterski, J. W., Ayala, P. Y., Morokuma, K., Voth, G. A., Salvador, P., Dannenberg, J. J., Zakrzewski, V. G., Dapprich, S., Daniels, A. D., Strain, M. C., Farkas, O., Malick, D. K., Rabuck, A. D., Raghavachari, K., Foresman, J. B., Ortiz, J. V., Cui, Q., Baboul, A. G., Clifford, S., Cioslowski, J., Stefanov, B. B., Liu, G., Liashenko, A., Piskorz, P., Komaromi, I., Martin, R. L., Fox, D. J., Keith, T., Al-Laham, M. A., Peng, C. Y., Nanayakkara, A., Challacombe, M., Gill, P. M. W., Johnson, B., Chen, W., Wong, M. W., Gonzalez, C., and Pople, J. A. (2003) Gaussian 03, Revision A.1, Gaussian, Inc., Pittsburgh, PA.
37. Jorgensen, W. L., Chandrasekhar, J., Madura, J. D., Impey, R. W., and Klein, M. L. (1983) Comparison of simple potential functions for simulating liquid water. *J. Chem. Phys. 79*, 926–935.
38. Essmann, U., Perera, L., Berkowitz, M. L., Darden, T., Lee, H., and Pedersen, L. G. (1995) A smooth particle mesh Ewald method. *J. Chem. Phys. 103*, 8577–8593.
39. Braman, J., Papworth, C., and Greener, A. (1996) Site-directed mutagenesis using double-stranded plasmid DNA templates. *Methods Mol. Biol. 57*, 31–44.
40. Masson, P., Xie, W., Froment, M.-T., Levitsky, V., Fortier, P.-L., Albaret, C., and Lockridge, O. (1999) Interaction between the peripheral site residues of human butyrylcholinesterase, D70 and Y332, in binding and hydrolysis of substrates. *Biochim. Biophys. Acta 1433*, 281–293.
41. Sun, H., Shen, M. L., Pang, Y. P., Lockridge, O., and Brimijoin, S. (2002) Cocaine metabolism accelerated by a re-engineered human butyrylcholinesterase. *J. Pharmacol. Exp. Ther. 302*, 710–716.